Inhibition of adenovirus infection by mifepristone

José A. Marrugal-Lorenzo[†,1], Ana Serna-Gallego[†,1], Loreto González-González[1], Maria Buñuales[2,3], Joanna Poutou[2], Jerónimo Pachón[1,4], Manuela Gonzalez-Aparicio[2,3], Ruben Hernandez-Alcoceba[2,3*] and Javier Sánchez-Céspedes[1,4*]

[1]Institute of Biomedicine of Seville (IBiS), University Hospital Virgen del Rocío/CSIC/University of Seville, Clinical Unit of Infectious Diseases, Microbiology, and Preventive Medicine, Seville, Spain, [2] Gene Therapy Unit CIMA, Foundation for Applied Medical Research, University of Navarra, Pamplona, Spain, [3]Navarra Institute for Health Research (IdiSNA), and [4]Department of Medicine, University of Seville, Seville, Spain.

*Corresponding authors: Mailing address: Infectious Diseases Research Group, Institute of Biomedicine of Seville (IBiS). University of Seville/CSIC/University Hospital Virgen del Rocío, 41013, Seville, Spain, Tel: +34 955 923 104, *E-mail address*: jsanchez-ibis@us.es (J. Sanchez-Cespedes); Mailing address: Gene Therapy Unit CIMA, Foundation for Applied Medical Research, University of Navarra, 31008, Pamplona, Spain, Tel: +34 948 194 700, *E-mail address*: rubenh@unav.es (R. Hernández-Alcoceba)

[†]J.A.M.L. and A.S.G. contributed equally to this work

Running title: Mifepristone block HAdV infection

Abstract

The repurposing of drugs approved by the regulatory agencies for other indications is emerging as a valuable alternative for the development of new antimicrobial therapies, involving lower risks and costs than the *de novo* development of novel antimicrobial drugs. Adenovirus infections have showed a steady increment in recent years, with a high clinical impact in both immunosuppressed and immunocompetent patients. In this context, the lack of a specific drug to treat these infections supports the search for new therapeutic alternatives. In this study, we examined the anti-HAdV properties of mifepristone, a commercially available synthetic steroid drug. Mifepristone showed significant *in vitro* anti-HAdV activity at low micromolar concentrations with little cytotoxicity. Our mechanistic assays suggest that this drug could affect the microtubule transport, interfering with the entry of the virus into the nucleus and therefore inhibiting HAdV infection.

Keywords: Adenovirus; Antiviral drug; Mifepristone

1. Introduction

To date the Human Adenovirus Working Group (HAdV) reports the existence of 90 human adenovirus (HAdV) types grouped into seven species (A–G) (HAdV_Working_Group, 2018). In immunosuppressed patients, especially in children, the high clinical impact of HAdV infections and diseases is well documented, showing high morbidity and mortality (Echavarria, 2008; Lion, 2014; Wiegering et al., 2011; Wong et al., 2008). Moreover, although the incidence of HAdV community-acquired pneumonia (CAP) in immunocompetent individuals appear to be low, with the advances in molecular techniques of diagnosis during last years, HAdV infections have been increasingly found to be involve in occasional cases and outbreaks in healthy adults (Jonnalagadda et al., 2017; Kajon and Ison, 2016; Tan et al., 2016a; Tan et al., 2016b; Yoon et al., 2017; Yu et al., 2015). Despite this significant clinical impact there are no currently approved antiviral therapies to treat HAdV infections and the broadly acting antivirals available in the clinic show no satisfactory efficacy or safety against HAdV infections (Martinez-Aguado et al., 2015). Safe and efficient anti-HAdV drugs could also become a valuable antidote for the new class of anticancer agents based on replication-competent HAdV (Baker et al., 2018).

The repositioning of drugs that have been previously approved by the regulatory agencies for other indications is a valuable alternative for the development of new antimicrobial therapies, involving lower risks and costs than the *de novo* development of novel antimicrobial drugs (Cheng et al., 2016; Pietschmann, 2016; Soo et al., 2016). In this way, mifepristone (MIF, RU486), a synthetic steroid that is structurally close-related to progesterone and glucocorticoids (Figure 2A) and an US Food and Drug Administration (FDA)-approved drug, has been used for many years for the medical termination of intrauterine pregnancy (Vayssiere et al., 2018). In addition, there is an

increasing interest on the use of this drug against Cushing's disease and several types of cancer (Cuevas-Ramos et al., 2016; Grunberg et al., 2006). Therefore, there is wide clinical experience demonstrating the safety of this drug following acute and chronic regimes at high doses. This molecule has also been specifically evaluated as an activator in drug-dependent inducible systems to control expression of potentially toxic transgenes such as interleukin-12 (IL12) for the treatment of cancer (Parra-Guillen et al., 2013; Poutou et al., 2017). These pre-clinical studies using HAdV-derived gene therapy vectors gave us the opportunity to explore potential interferences between MIF and HAdV infection. In this work we describe for the first time that MIF inhibits HAdV infection in mice, and provide a potential mechanism of action taking place in human cells. Our results susggest that MIF should be formally tested as repurposed drug for the treatment of HAdV infections.

2. Material and methods

2.1 .Cells and viruses

Human A549 and HEK-293 and MRC-5 cell lines were from the American Type Culture Collection (ATCC, Manassas, VA). The 293β5 stable cell line overexpressing the human β5 integrin subunit was a kindly provided by Dr. Glen Nemerow (Nepomuceno et al., 2007; Nguyen et al., 2010). These cell lines were propagated in Dulbecco's modified Eagle medium (DMEM, Life Technologies/Thermo Fisher) supplemented with 10% fetal bovine serum (FBS) (Omega Scientific, Tarzana, CA), 10 mM HEPES, 4 mM L-glutamine, 100 units/ml penicillin, 100 μg/ml streptomycin, and 0.1 mM non-essential amino acids (complete DMEM).

Wild-type HAdV5, HAdV16, HAdV19 and cytomegalovirus (HCMV) were obtained from the ATCC. The HAdV5-GFP used in this work is replication-defective virus

containing a CMV promoter-driven enhanced green fluorescent protein (eGFP) reporter gene cassette in place of the E1/E3 regions (Nepomuceno et al., 2007). HAdV were propagated in 293β5 cells and isolated from cellular lysate by cesium chloride density centrifugation. Virus concentration (mg/ml) was calculated with the Bio-Rad Protein Assay (Bio-Rad Laboratories) and converted to virus particles/ml (vp/ml) using 4×10^{12} vp/mg.

Ad-CMV-Luc is a first-generation HAdV-5 vector purchased from Vector Biolabs (Malvern, PA, USA) and amplified in HEK-293 cells. Purification was carried out by cesium chloride density centrifugation and subsequent desalting in Sepharose columns. Virus quantification was performed using the Adeno-X rapid titer kit (Clontech, Mountain View, CA, USA).

2.2. Cytotoxicity assay

The cytotoxicity of the MIF was measured using the Alamar Blue Cell Viability Assay (Invitrogen) according to the manufacturer's instructions. Actively dividing A549 cells were incubated with the drug for 48 h. After the incubation the Alamar Blue reagent was added to the cells (1/10th Alamar Blue reagent in culture medium) for an extra 4 h. The 50% cytotoxic concentration (CC_{50}) of the MIF was calculated according to Cheng *et al.* (Cheng et al., 2002). The selectivity index (SI) was evaluated as the ratio of CC_{50} to IC_{50}, where the IC_{50} is defined as the concentration of compound that inhibits HAdV infection by 50%.

2.3. HAdV plaque assay

For low MOI infections, MIF was tested in a dose-response assay using 0.06 vp/cell and concentrations ranging from 10 to 0.62 μM in a plaque assay. Briefly, 293β5 cells were seeded in 6-well plates at a density of 4×10^5 cells per well in duplicate for each condition. When cells reached 80−90% confluency, they were infected with HAdV5-

GFP (0.06 vp/cell) and rocked for 2 h at 37°C. After the incubation the inoculum was removed, and the cells were washed once with PBS. The cells were then carefully overlaid with 4 mL/well of equal parts of 1.6% (water/vol) Difco Agar Noble (Becton, Dickinson & Co., Sparks, MD) and 2× EMEM (Minimum Essential Medium Eagle, BioWhittaker) supplemented with 2×penicillin/streptomycin, 2× L-glutamine, and 10% FBS. The mixture also contained the drug in concentrations ranging from 10 to 0.62 μM Following incubation for 7 days at 37°C, plates were scanned with a Typhoon 9410 imager (GE Healthcare Life Sciences) and plaques were quantified with ImageJ (Schneider et al., 2012).

2.4. Virus yield reduction

The effect of the MIF on virus production was evaluated in a burst assay. A549 cells were infected with wild-type HAdV5, HAdV16 and HAdV19 in the presence or absence of 50 μM of the drug. After 48 h, cells were harvested and subjected to three rounds of freeze/thaw. Serial dilutions of clarified lysates were titrated on A549 cells, and TCID50 values were calculated using an end-point dilution method (Reed and Muench, 1938).

2.5. HAdV entry assay

The anti-HAdV activity was initially measured in an entry assay using human A549 epithelial cells (3×10^5 cells/well in corning black wall, clear bottom 96-well plates) infected with HAdV-GFP (2000 vp/cell) in the presence of the MIF using serial dilutions ranging from 120 to 1.87μM. Virus was preincubated with the drug for 45 min at 4°C, and then added to cells. A standard infection curve was generated in parallel by infecting cells in the absence of the drug using serial 2-fold dilutions of virus. All reactions were done in triplicate. Cells, virus, and MIF were incubated for 48 h at 37°C and 5% CO_2. Infection, as measured by HAdV-mediated GFP expression, was analyzed

using a Typhoon 9410 imager (GE Healthcare Life Sciences) and quantified with ImageQuantTL (GE Healthcare Life Sciences).

2.6. HAdV-mediated endosome disruption

To assess endosomal escape, HAdV-mediated ribotoxin (α-sarcin) delivery assays were performed as previously described (Moyer et al., 2011) with some modifications. Briefly, 30,000 A549 cells were seeded in black 96-well plates and incubated in complete DMEM for 24 h. Cells were washed and then incubated at 37°C for 1 h in DMEM without cysteine or methionine and supplemented with 10% FBS (DMEM-). In parallel, 3-fold serial dilutions (333–0.15 ng) of Ad5ts1 or HAdV5 wt was preincubated with cells in the presence of 50 μM of MIF or the same volume of DMSO (control) for 1 h on ice. Following the incubations, the medium was removed and replaced with 50 ml DMEM-containing 0.1 mg/ml of α-sarcin (Calbiochem/EMD Biosciences, La Jolla, CA) and the virus/drug mixtures, and incubated for 2 h at 37°C. Nascent protein synthesis analysis was performed using the Click-iT HPG Alexa Fluor 488 Protein Synthesis Assay Kits (Invitrogen) according to the manufacturer's instructions. After incubation with Click-iT reaction buffer containing Alexa Fluor 488 azide, L-homopropargylglycine (HPG) (amino acid analog of methionine) incorporation was measured using a Typhoon 9410 imager (GE Healthcare Life Sciences) and calculated by subtracting the background level of a control well containing L-homopropargylglycine (HPG) and α-sarcin but not virus.

2.7. HAdV DNA quantification by real-time PCR

For DNA quantification, A549 cells (150,000 cells/well in a 24-well plate) were infected with wild-type HAdV5 (100 vp/cell) and incubated for 2 h at 37°C in complete DMEM. After the incubation, excess virus was removed and the medium was replaced with 500 μL of complete DMEM containing 50 μM of MIF or the same volume of

DMSO (positive control). All samples were done in triplicate. After 24 h of incubation at 37°C and 5% CO_2, DNA was purified from the cell lysate with the QIAamp DNA Mini Kit (QIAGEN, Valencia, CA) following the manufacturer's instructions. TaqMan primers and probes for a region of the HAdV5 hexon were designed with the GenScript Real-Time PCR (TaqMan) Primer Design software (GenScript). Oligonucleotides sequences were AdF, 5′-GACATGACTTTTGAGGTGGA-3′; AdR, 5′-GTGGCGTTGCCGGCCGAGAA-3′; and AdProbe, 5′-TCCATGGGATCCACCTCAAA-3′. Real-time PCR mixtures consisted of 2 μL of the purified DNA, AdF, and AdR at a concentration of 200 nM each and AdProbe at a concentration of 50 nM in a total volume of 12.5 μL and mixed with 12.5 μL of KAPA PROBE FAST qPCR Master Mix (KAPABiosystems, MA). The PCR cycling protocol was 95°C for 3 min followed by 40 cycles of 95°C for 10 s and 60°C for 30 s.

Human glyceraldehyde-3-phosphate dehydrogenase (GAPDH) gene was used as internal control. Oligonucleotides sequences for GAPDH and conditions were those previously reported by Rivera *et al.* (Rivera et al., 2004). For quantification, gene fragments from hexon, and GAPDH were cloned into the pGEM-T Easy vector (Promega) and known concentrations of template were used to generate a standard curve in parallel for each experiment. All assays were performed in a C1000 thermal cycler apparatus (BioRad).

2.8. Nuclear-associated HAdV genomes

Nuclear delivery of the HAdV genome was assessed with real-time PCR following nuclear isolation from infected cells using a previously described protocol with a few modifications (Schreiner et al., 2012). Briefly, 1×10^6 A549 cells in 6-well plates were infected with HAdV5 wild-type at MOI 2,000 vp/cell in the presence of 50 μM of MIF or the same volume of DMSO. Forty-five min after the infection, cytoplasmic and

nuclear fractions were separated using a hypotonic buffer solution and NP-40 detergent. Following infection, A549 cells were trypsinized and collected and then washed twice with PBS. The cell pellet was resuspended in 500 µL of 1×hypotonic buffer (20 mM Tris-HCl pH 7.4, 10 mM NaCl, 3 mM MgCl2) and incubated for 15min at 4°C. Then, 25 µL of NP-40 was added and the samples were vortexed. The homogenates were centrifuged for 10 min at 835g at 4°C. Following removal of the cytoplasmic fraction (supernatant), DNA was isolated from the nuclear fraction (pellet) using the QIAamp DNA Mini Kit (QIAGEN, Valencia, CA).

2.9. HCMV infectivity assay by quantitative PCR

To test the sensitivity of HCMV to MIF, MRC-5 cells (1.75×10^5 cells/well in a 6-well plate) were infected with HCMV at a MOI of 0.05 vp/cell and incubated in complete DMEM supplemented with 50 µM of MIF or the same volume of DMSO in triplicate. After 72h of incubation at 37 °C and 5% CO_2, HCMV DNA was purified from the cell lysate with the QIAamp DNA Mini Kit (Qiagen, Valencia, CA) following the manufacturer's instructions. Real-time PCR primers, mixtures and protocols were the same as previously reported (Sanchez-Cespedes et al., 2016).

2.10. In vivo experiments

Female C57BL6/J mice (Harlan Iberica, Barcelona, Spain) were treated with daily intraperitoneal administration of 4 mg/Kg MIF (Sigma, St. Louis, MO, USA) dissolved in 70 µl of sesame oil (Sigma) for 10 consecutive days. On the last day, mice received a single intravenous administration of Ad-CMV-Luc ($2x10^8$ iu). For *in vivo* analysis of luciferase activity, mice were anesthetized with intraperitoneal injection of a ketamine/xylacine mixture. The substrate D-luciferin (REGIS Technologies, Chicago, IL, USA) was administered intraperitoneally (100 µl of a 30 µg/µl solution in PBS) and 5 minutes later light emission was detected using a PhotonImager Optima apparatus

(BioSpace, Paris, France). Data were analyzed using the M3Vision software (BioSpace). At the end of the observation period, mice were sacrificed and liver samples were frozen in liquid nitrogen and DNA was isolated using QIAmp DNA Mini Kit (Qiagen, Hilden, Germany) according to the manufacturer's instructions. qRT-PCR of viral genomes was performed as described before. All animal work was performed following protocols approved by the local ethical committee.

2.11. Statistical Analyses

Statistical analyses were performed with the GraphPad Prism 5 suite using one-way analysis of variance (ANOVA). For the animal tests, differences between control and MIF-treated groups were analyzed using the Mann Whitney U test. Unless otherwise indicated, data are presented as the mean of triplicate samples ± standard deviation (SD). P-values are indicated when statistically significant.

3. Results

3.1. Inhibition of HAdV infection by MIF in mice.

In the course of our pre-clinical evaluation of HAdV-based vectors carrying reporter genes, we detected interference between MIF and vector transduction in the liver of mice. Mice pre-treated with intraperitoneal MIF using different schedules showed a significant inhibition of transgene expression. In particular, pre-treatment of mice with 4 mg/Kg MIF led to a significant inhibition of transgene expression when the animals received intravenous administration of the first-generation HAdV vector Ad-CMV-Luc, in comparison with untreated mice (Figure 1A). Analysis of the viral load in liver samples from these animals confirmed a reduction in viral copies in the liver, consistent with reduced HAdV entry (Figure 1B). In contrast, sustained expression of luciferase mediated by a High-Capacity HAdV vector (Poutou et al., 2017) was not affected when

MIF was administered after virus administration (data not shown), ruling out the possibility of inhibition at the level of reporter protein synthesis or stability. These observations suggested an inhibition of HdAV infection and prompted us to perform a specific evaluation of the anti-HAdV properties of MIF and to characterize its mechanism of action with the final aim to explore its potential as repurposed drug for the treatment of HAdV infections.

3.2. Anti-adenovirus activity of MIF

First, we performed a classical plaque forming assay using the HAdV5-GFP virus on 293β5 cells. MIF showed a dose-dependent anti-HAdV activity at low MOI of virus (0.06 vp/cell), with 100% inhibition of plaque formation at concentrations higher than 5 μM. We next evaluated the anti-HAdV effect of the drug using a virus burst assay which measures the production of virus particles. Treatment with MIF was associated with more than 100-fold reduction in virus yield of different HAdV types (239.2±39.4, 160.5±30.2 and 243.6±33.6–fold for HAdV5, HAdV16 and HAdV19 respectively). We also analyzed the cellular cytotoxicity of MIF. At concentrations <50 μM, MIF did not significantly alter cell viability as determined by the Alamar Blue Cell Viability Assay. The CC_{50} for MIF was 270.2 μM, significantly higher than 50 μM concentration used in our antiviral and mechanistic assays. Results of the IC_{50}, CC_{50}, selective index and yield reduction for MIF against HAdV5 are shown in Table 1.

3.3. Impact on HAdV entry

MIF showed a significant inhibition of HAdV5-GFP entry in human A549 cells (Figure 2B), with an IC_{50} value of 16.22±0.81 μM. As we reported in a previous work, the results obtained with this entry assay do not give conclusive indications of their potential mechanism of action (Sanchez-Cespedes et al., 2014).

After binding and internalization of the HAdV, inside the endosome, the exposure of protein VI induces endosome lysis, and the partially uncoated HAdV capsid escape. Once in the cytosol it is transported to the nuclear membrane by the microtubule network. We evaluated MIF in a physiological assay involving HAdV-mediated co-delivery of α-sarcin in live cells as an indication of the ability of MIF to influence virus-mediated endosomolysis (Sanchez-Cespedes et al., 2014; Wiethoff et al., 2005). We did not detect a significant change in the ID_{50} (50% inhibitory dose) for HAdV-mediated endosome penetration in the presence of MIF compared to the DMSO control (Figure 2C). In contrast, the endosome penetration-defective mutant virus Ad5ts1 exhibited a 23-fold increase in the ID_{50} with respect to the DMSO control (Figure 2C).

To clarify if this drug was able to block some of the steps of the entry pathway, we carried out an assay to quantitatively measure the HAdV genome accessibility to the nucleus. Inside the endosome, after binding and internalization of the HAdV particle, the exposure of protein VI triggers endosome lysis, after which the partially uncoated HAdV capsid is transported to the nuclear envelope where the HAdV genome is imported into the nucleus through the nuclear pore complex (Strunze et al., 2011). We evaluated the nuclear delivery of the HAdV genome carrying out an assay to quantitatively measure the HAdV genome accessibility to the nucleus (Schreiner et al., 2012). As reflected in Figure 3A, MIF showed a significant reduction in the amount of HAdV genomes isolated from the nucleus of cells treated with the drug versus those treated with DMSO at 45 min post-infection. We also measured the DNA copy number of the cellular housekeeping gene GAPDH in both the nucleus and the cytoplasm as a control for the purity of nuclear isolation (Figure 3B). Our results indicated that we were specifically measuring the HAdV DNA that reached the nucleus and that MIF

blocked partially HAdV genome accessibility to the nucleus because only 43,7% ± 4,3 of the viral genomes acceded to the nucleus of the cell, compared with untreated cells.

3.4. Impact on HAdV replication

We performed quantitative real-time PCR (qPCR) to measure HAdV DNA replication in the presence of the MIF. To avoid the interference of newly generated viral particles derived from subsequent rounds of infection occurring 32−36 h post infection, DNA was extracted 24 h post-infection (Horwitz, 1991). As we did in previous works, quantitative PCR was used to quantify the generation of newly HAdV DNA copies synthetized in a single round of infection as a measure of DNA replication efficiency. The presence of the drug (50 μM) significantly inhibited HAdV5 DNA replication by more than 50% ($p < 0.05$, Dunnett's Multiple Comparison test), with no significant effect on the cellular control gene GAPDH (Figure 4A). The decrease in HAdV DNA copy number at the nucleus 24 hpi in the presence of MIF suggested several possibilities for its precise mechanism of inhibition.

3.5. MIF restricts HCMV infection

Given that other antiviral compounds such as piperazine derivatives or nucleotide and nucleoside analogues have been shown to have broad activity against multiple dsDNA virus including HCMV and HAdV by different mechanisms (Lindemans et al., 2010; Sanchez-Cespedes et al., 2016), we explored the possible inhibitory activity of MIF on HCMV DNA replication. Quantification of total HCMV DNA 72 h after infection of MRC-5 cells revealed significant differences between samples treated with our drug and those treated with the same volume of DMSO (Figure 4B). Quantitative PCR for the GAPDH gene was included as control, again showing no differences between samples (data not shown).

4. Discussion and conclusions

The goal of this work was to confirm the potential anti-HAdV activity of MIF, discovered upon a serendipitous observation in the pre-clinical evaluation of inducible systems delivered by HAdV vectors in mice.

Our results show that MIF exerts a significant anti-HAdV activity at low micromolar concentrations with low cytotoxicity at low and high MOIs. It has a broad antiviral activity with significant overall reduction in HAdV yield for HAdV5 (HAdV family C), HAdV16 (HAdV family B) and HAdV19 (HAdV family D) and significant inhibition of CMV infection.

As for MIF mechanism of action, we have confirmed that it interferes with HAdV genome accessibility into the nucleus. Furthermore, using a physiological assay involving HAdV-mediated co-delivery of α-sarcin in live cells as an indication of the ability of MIF to influence virus-mediated endosomolysis we did not detect a significant change in the ID50 (50% inhibitory dose) for HAdV-mediated endosome penetration in the presence of MIF compared to the control. We have confirmed that the presence of MIF has an impact on HAdV replication. There are two possible scenarios to explain this decrease in HAdV DNA copy number at the nucleus 24 hpi. First, MIF could alter the entry of the HAdV genome into the nucleus or, alternatively, in could inhibit HAdV DNA replication directly by interfering with a protein involved in this process, such as the HAdV DNA polymerase or, it may impact the transcription of the HAdV immediate early genes, which is a prerequisite for subsequent DNA replication. Our mechanistic assays suggest that MIF may be acting in the first of these scenarios, targeting early steps in HAdV life cycle, after viral escape from the endosome and before HAdV DNA translocation into the nucleus, which might be explained by an interference with the partially decapsidated viral particle transport by the microtubular network to the nuclear pores.

During entry, the HAdV capsid undergoes a series of interactions with the host cell before delivery of the viral genome into the nucleus. After receptor binding by the HAdV fiber, the viral particles are internalized by receptor-mediated endocytosis mediated by the interaction between the HAdV penton base and cellular αvβ3 or αvβ5 integrins (Smith et al., 2003; Tomko et al., 1997). Inside the endosome, the viral capsid undergoes partial disassembly and exposes several viral proteins, including the lytic protein VI which will trigger the endosomolysis and the subsequent virus release to the cytoplasm (Wiethoff et al., 2005). The partially uncoated HAdV capsid is then released into the cytoplasm and transported to the nuclear pore complex by the microtubular network (Smith et al., 2008; Wiethoff et al., 2005). Moreover, HAdV associates with microtubules following endosome penetration by the presence of microtubule-associated proteins (MAPs) and the block of this association can prevent HAdV infection (Bailey et al., 2003; Kelkar et al., 2004; Leopold et al., 2000; Luftig and Weihing, 1975; Smith et al., 2008; Suomalainen et al., 2001; Suomalainen et al., 1999). One example of the functional relevance of this process is the anti-hexon neutralizing antibody 9C12, a monoclonal antibody that blocks HAdV infection at the microtubule-dependent transport stage (Smith et al., 2008). Smith *et al.* suggested that the binding of 9C12 to HAdV could altered the association of the HAdV capsid with microtubules, describing a new mode of action for a neutralizing antibody to block infection by a non-enveloped virus (Smith et al., 2008). Based on the results obtained in this work we hypothesized that MIF could act in a similar way as 9C12, preventing the nuclear accumulation of HAdV genomes by hampering their transport from the endosome to the nuclear pore complex.

Repurposing of drugs for diseases other than those the drug was approved for is becoming a valuable alternative for drug development that reduces significantly the

high cost and the time-consuming of developing a new drug (Chong and Sullivan, 2007; De Rycker et al., 2016; Martinez-Romero and Garcia-Sastre, 2015; Perwitasari et al., 2015). In the case of MIF, many reports support their repositioning as potential anti-cancer drug since it has been showed to inhibit growth of many cancer cells as well as for the treatment of Cushing's syndrom (Chen et al., 2014; Morgan and Laufgraben, 2013; Parra-Guillen et al., 2013). As for its pharmacokinetics characteristics, both human and animal studies indicate that the initial steps of MIF metabolism, after absorption from the intestine into the liver portal vein, is primarily to metapristone, and the main metabolic enzymes responsible to the oxidation of MIF are cytochromes P450 3A4, and to a lesser extent, P450 3A5 (Chen et al., 2014; Jang et al., 1996; Khan et al., 2002). Different publications have reported plasma concentrations of MIF (*Cmax*) in human after single oral administration of MIF at different doses (25-600 mg), of up to 2.3 μM, a concentration value that is above the IC_{50} we found against HAdV (Lahteenmaki et al., 1987; Tang et al., 2009; Teng et al., 2011).

MIF has demonstrated to present a significant anti-HAdV and anti-CMV activity at low micromolar concentration and low cytotoxicity. Altogether, our findings support the further evaluation of this drug in an animal model of infection to confirm its efficacy and safety preventing HAdV diseases.

Conflicts of interest

The authors declare no conflicts of interest.

Acknowledgments

Supported by Plan Nacional de I+D+i 2013-2016 and Instituto de Salud Carlos III, Ministerio de Economía, Industria y Competitividad, Spanish Network for Research in

Infectious Diseases (REIPI RD16/0016/0009) – co-financed by "A way to achieve Europe" ERDF, the Instituto de Salud Carlos III, Proyectos de Investigaciónen Salud (PI15/00489), the Spanish Department of Science (SAF2015-65157-R) and the Spanish Adenovirus Network (AdenoNet, BIO2015/68990-REDT). J.S.C. is supported by the "Contract to Access to the Spanish System of Research and Innovation of the Program of R+D+i of the University of Seville" (USE-13901-D) grant.

References

Bailey, C.J., Crystal, R.G., Leopold, P.L., 2003. Association of adenovirus with the microtubule organizing center. Journal of virology 77, 13275-13287.

Baker, A.T., Aguirre-Hernandez, C., Hallden, G., Parker, A.L., 2018. Designer Oncolytic Adenovirus: Coming of Age. Cancers 10.

Cuevas-Ramos, D., Lim, D.S.T., Fleseriu, M., 2016. Update on medical treatment for Cushing's disease. Clinical diabetes and endocrinology 2, 16.

Chen, J., Wang, J., Shao, J., Gao, Y., Xu, J., Yu, S., Liu, Z., Jia, L., 2014. The unique pharmacological characteristics of mifepristone (RU486): from terminating pregnancy to preventing cancer metastasis. Medicinal research reviews 34, 979-1000.

Cheng, F., Murray, J.L., Rubin, D.H., 2016. Drug Repurposing: New Treatments for Zika Virus Infection? Trends in molecular medicine.

Cheng, H.Y., Lin, C.C., Lin, T.C., 2002. Antiherpes simplex virus type 2 activity of casuarinin from the bark of Terminalia arjuna Linn. Antiviral research 55, 447-455.

Chong, C.R., Sullivan, D.J., Jr., 2007. New uses for old drugs. Nature 448, 645-646.

De Rycker, M., Thomas, J., Riley, J., Brough, S.J., Miles, T.J., Gray, D.W., 2016. Identification of Trypanocidal Activity for Known Clinical Compounds Using a New Trypanosoma cruzi Hit-Discovery Screening Cascade. PLoS neglected tropical diseases 10, e0004584.

Echavarria, M., 2008. Adenoviruses in immunocompromised hosts. Clinical microbiology reviews 21, 704-715.

Grunberg, S.M., Weiss, M.H., Russell, C.A., Spitz, I.M., Ahmadi, J., Sadun, A., Sitruk-Ware, R., 2006. Long-term administration of mifepristone (RU486): clinical tolerance during extended treatment of meningioma. Cancer investigation 24, 727-733.

HAdV_Working_Group, 2018. http://hadvwg.gmu.edu/.

Horwitz, M.S., 1991. Adenoviridae and their replication, in: virology, F. (Ed.), Fields, B. N., Knipe, D. M., Chanock, R. M., et al. , 2nd ed. Raven Press, New York, NY, pp. 771-813.

Jang, G.R., Wrighton, S.A., Benet, L.Z., 1996. Identification of CYP3A4 as the principal enzyme catalyzing mifepristone (RU 486) oxidation in human liver microsomes. Biochemical pharmacology 52, 753-761.

Jonnalagadda, S., Rodriguez, O., Estrella, B., Sabin, L.L., Sempertegui, F., Hamer, D.H., 2017. Etiology of severe pneumonia in Ecuadorian children. PloS one 12, e0171687.

Kajon, A.E., Ison, M.G., 2016. Severe Infections with Human Adenovirus 7d in 2 Adults in Family, Illinois, USA, 2014. Emerging infectious diseases 22, 730-733.

Kelkar, S.A., Pfister, K.K., Crystal, R.G., Leopold, P.L., 2004. Cytoplasmic dynein mediates adenovirus binding to microtubules. Journal of virology 78, 10122-10132.

Khan, K.K., He, Y.Q., Correia, M.A., Halpert, J.R., 2002. Differential oxidation of mifepristone by cytochromes P450 3A4 and 3A5: selective inactivation of P450 3A4. Drug metabolism and disposition: the biological fate of chemicals 30, 985-990.

Lahteenmaki, P., Heikinheimo, O., Croxatto, H., Spitz, I., Shoupe, D., Birgerson, L., Luukkainen, T., 1987. Pharmacokinetics and metabolism of RU 486. Journal of steroid biochemistry 27, 859-863.

Leopold, P.L., Kreitzer, G., Miyazawa, N., Rempel, S., Pfister, K.K., Rodriguez-Boulan, E., Crystal, R.G., 2000. Dynein- and microtubule-mediated translocation of adenovirus serotype 5 occurs after endosomal lysis. Human gene therapy 11, 151-165.

Lindemans, C.A., Leen, A.M., Boelens, J.J., 2010. How I treat adenovirus in hematopoietic stem cell transplant recipients. Blood 116, 5476-5485.

Lion, T., 2014. Adenovirus infections in immunocompetent and immunocompromised patients. Clinical microbiology reviews 27, 441-462.

Luftig, R.B., Weihing, R.R., 1975. Adenovirus binds to rat brain microtubules in vitro. Journal of virology 16, 696-706.

Martinez-Aguado, P., Serna-Gallego, A., Marrugal-Lorenzo, J.A., Gomez-Marin, I., Sanchez-Cespedes, J., 2015. Antiadenovirus drug discovery: potential targets and evaluation methodologies. Drug discovery today 20, 1235-1242.

Martinez-Romero, C., Garcia-Sastre, A., 2015. Against the clock towards new Ebola virus therapies. Virus research 209, 4-10.

Morgan, F.H., Laufgraben, M.J., 2013. Mifepristone for management of Cushing's syndrome. Pharmacotherapy 33, 319-329.

Moyer, C.L., Wiethoff, C.M., Maier, O., Smith, J.G., Nemerow, G.R., 2011. Functional genetic and biophysical analyses of membrane disruption by human adenovirus. Journal of virology 85, 2631-2641.

Nepomuceno, R.R., Pache, L., Nemerow, G.R., 2007. Enhancement of gene transfer to human myeloid cells by adenovirus-fiber complexes. Molecular therapy : the journal of the American Society of Gene Therapy 15, 571-578.

Nguyen, E.K., Nemerow, G.R., Smith, J.G., 2010. Direct evidence from single-cell analysis that human {alpha}-defensins block adenovirus uncoating to neutralize infection. Journal of virology 84, 4041-4049.

Parra-Guillen, Z.P., Janda, A., Alzuguren, P., Berraondo, P., Hernandez-Alcoceba, R., Troconiz, I.F., 2013. Target-mediated disposition model describing the dynamics of IL12 and IFNgamma after administration of a mifepristone-inducible adenoviral vector for IL-12 expression in mice. The AAPS journal 15, 183-194.

Perwitasari, O., Yan, X., O'Donnell, J., Johnson, S., Tripp, R.A., 2015. Repurposing Kinase Inhibitors as Antiviral Agents to Control Influenza A Virus Replication. Assay and drug development technologies 13, 638-649.

Pietschmann, T., 2016. Clinically approved ion channel inhibitors close gates for hepatitis C virus -and open doors for drug repurposing in viral infectious diseases. Journal of virology.

Poutou, J., Bunuales, M., Gonzalez-Aparicio, M., German, B., Zugasti, I., Hernandez-Alcoceba, R., 2017. Adaptation of vectors and drug-inducible systems for controlled expression of transgenes in the tumor microenvironment. Journal of controlled release : official journal of the Controlled Release Society 268, 247-258.

Reed, L.V., Muench, H., 1938. A simple method of stimating fifty percent endpoints. American Journal of Hygiene 27, 4.

Rivera, A.A., Wang, M., Suzuki, K., Uil, T.G., Krasnykh, V., Curiel, D.T., Nettelbeck, D.M., 2004. Mode of transgene expression after fusion to early or late viral genes of a conditionally replicating adenovirus via an optimized internal ribosome entry site in vitro and in vivo. Virology 320, 121-134.

Sanchez-Cespedes, J., Martinez-Aguado, P., Vega-Holm, M., Serna-Gallego, A., Candela, J.I., Marrugal-Lorenzo, J.A., Pachon, J., Iglesias-Guerra, F., Vega-Perez, J.M., 2016. New 4-Acyl-1-phenylaminocarbonyl-2-phenylpiperazine Derivatives as Potential Inhibitors of Adenovirus Infection. Synthesis, Biological Evaluation, and Structure-activity Relationships. Journal of medicinal chemistry 59, 5432-5448.

Sanchez-Cespedes, J., Moyer, C.L., Whitby, L.R., Boger, D.L., Nemerow, G.R., 2014. Inhibition of adenovirus replication by a trisubstituted piperazin-2-one derivative. Antiviral research 108, 65-73.

Schneider, C.A., Rasband, W.S., Eliceiri, K.W., 2012. NIH Image to ImageJ: 25 years of image analysis. Nature methods 9, 671-675.

Schreiner, S., Martinez, R., Groitl, P., Rayne, F., Vaillant, R., Wimmer, P., Bossis, G., Sternsdorf, T., Marcinowski, L., Ruzsics, Z., Dobner, T., Wodrich, H., 2012. Transcriptional activation of the adenoviral genome is mediated by capsid protein VI. PLoS pathogens 8, e1002549.

Smith, J.G., Cassany, A., Gerace, L., Ralston, R., Nemerow, G.R., 2008. Neutralizing antibody blocks adenovirus infection by arresting microtubule-dependent cytoplasmic transport. Journal of virology 82, 6492-6500.

Smith, T.A., Idamakanti, N., Rollence, M.L., Marshall-Neff, J., Kim, J., Mulgrew, K., Nemerow, G.R., Kaleko, M., Stevenson, S.C., 2003. Adenovirus serotype 5 fiber shaft influences in vivo gene transfer in mice. Human gene therapy 14, 777-787.

Soo, V.W., Kwan, B.W., Quezada, H., Castillo-Juarez, I., Perez-Eretza, B., Garcia-Contreras, S.J., Martinez-Vazquez, M., Wood, T.K., Garcia-Contreras, R., 2016. Repurposing of Anticancer Drugs for the Treatment of Bacterial Infections. Current topics in medicinal chemistry.

Strunze, S., Engelke, M.F., Wang, I.H., Puntener, D., Boucke, K., Schleich, S., Way, M., Schoenenberger, P., Burckhardt, C.J., Greber, U.F., 2011. Kinesin-1-mediated capsid disassembly and disruption of the nuclear pore complex promote virus infection. Cell host & microbe 10, 210-223.

Suomalainen, M., Nakano, M.Y., Boucke, K., Keller, S., Greber, U.F., 2001. Adenovirus-activated PKA and p38/MAPK pathways boost microtubule-mediated nuclear targeting of virus. The EMBO journal 20, 1310-1319.

Suomalainen, M., Nakano, M.Y., Keller, S., Boucke, K., Stidwill, R.P., Greber, U.F., 1999. Microtubule-dependent plus- and minus end-directed motilities are competing processes for nuclear targeting of adenovirus. The Journal of cell biology 144, 657-672.

Tan, D., Fu, Y., Xu, J., Wang, Z., Cao, J., Walline, J., Zhu, H., Yu, X., 2016a. Severe adenovirus community-acquired pneumonia in immunocompetent adults: chest radiographic and CT findings. Journal of thoracic disease 8, 848-854.

Tan, D., Zhu, H., Fu, Y., Tong, F., Yao, D., Walline, J., Xu, J., Yu, X., 2016b. Severe Community-Acquired Pneumonia Caused by Human Adenovirus in Immunocompetent Adults: A Multicenter Case Series. PloS one 11, e0151199.

Tang, C., Bi, H.C., Zhong, G.P., Chen, X., Huang, Z.Y., Huang, M., 2009. Simultaneous determination of mifepristone and monodemethyl-mifepristone in human plasma by liquid chromatography-tandem mass spectrometry method using levonorgestrel as an internal standard: application to a pharmacokinetic study. Biomedical chromatography : BMC 23, 71-80.

Teng, Y.N., Dong, R.Q., Wang, B.J., Liu, H.J., Jiang, Z.M., Wei, C.M., Zhang, R., Yuan, G.Y., Liu, X.Y., Guo, R.C., 2011. Determinations of mifepristone and its metabolites and their pharmacokinetics in healthy female Chinese subjects. Yao xue xue bao = Acta pharmaceutica Sinica 46, 1241-1245.

Tomko, R.P., Xu, R., Philipson, L., 1997. HCAR and MCAR: the human and mouse cellular receptors for subgroup C adenoviruses and group B coxsackieviruses. Proceedings of the National Academy of Sciences of the United States of America 94, 3352-3356.

Vayssiere, C., Gaudineau, A., Attali, L., Bettahar, K., Eyraud, S., Faucher, P., Fournet, P., Hassoun, D., Hatchuel, M., Jamin, C., Letombe, B., Linet, T., Msika Razon, M., Ohanessian, A., Segain, H., Vigoureux, S., Winer, N., Wylomanski, S., Agostini, A.,

2018. Elective abortion: Clinical practice guidelines from the French College of Gynecologists and Obstetricians (CNGOF). European journal of obstetrics, gynecology, and reproductive biology 222, 95-101.

Wiegering, V., Kaiser, J., Tappe, D., Weissbrich, B., Morbach, H., Girschick, H.J., 2011. Gastroenteritis in childhood: a retrospective study of 650 hospitalized pediatric patients. International journal of infectious diseases : IJID : official publication of the International Society for Infectious Diseases 15, e401-407.

Wiethoff, C.M., Wodrich, H., Gerace, L., Nemerow, G.R., 2005. Adenovirus protein VI mediates membrane disruption following capsid disassembly. Journal of virology 79, 1992-2000.

Wong, S., Pabbaraju, K., Pang, X.L., Lee, B.E., Fox, J.D., 2008. Detection of a broad range of human adenoviruses in respiratory tract samples using a sensitive multiplex real-time PCR assay. Journal of medical virology 80, 856-865.

Yoon, B.W., Song, Y.G., Lee, S.H., 2017. Severe community-acquired adenovirus pneumonia treated with oral ribavirin: a case report. BMC research notes 10, 47.

Yu, H.X., Zhao, M.M., Pu, Z.H., Wang, Y.Q., Liu, Y., 2015. Clinical data analysis of 19 cases of community-acquired adenovirus pneumonia in immunocompetent adults. International journal of clinical and experimental medicine 8, 19051-19057.

Table 1. CC_{50}, IC_{50}, SI and yield reduction values for MIF.

	CC_{50} (µM)	**IC_{50} (µM)**	**Selectivity Index (SI)**	**Yield reduction (fold-reduction)**
MIF	270.2±17.5	1.9±0.8	142.2	239.2±39.4

Figure 1. MIF inhibits infection of HAdV-based vectors carrying a luciferase reporter gene in mice. C57BL/6 mice were treated with daily intraperitoneal administrations of MIF (4 mg/Kg) during 10 days. The last day of treatment, Ad-CMV-Luc ($2x10^8$ iu) was injected intravenously. A control group of mice received the same dose of virus but no MIF treatment (MIF). Lucifease expression was determined by bioluminescence imaging at the indicated times, and is represented as light emission (photons/sec) in the abdominal area **(A)**. Animal were then sacrificed to determine viral copies in the liver, relative to the GAPDH endogenous gene **(B)**.

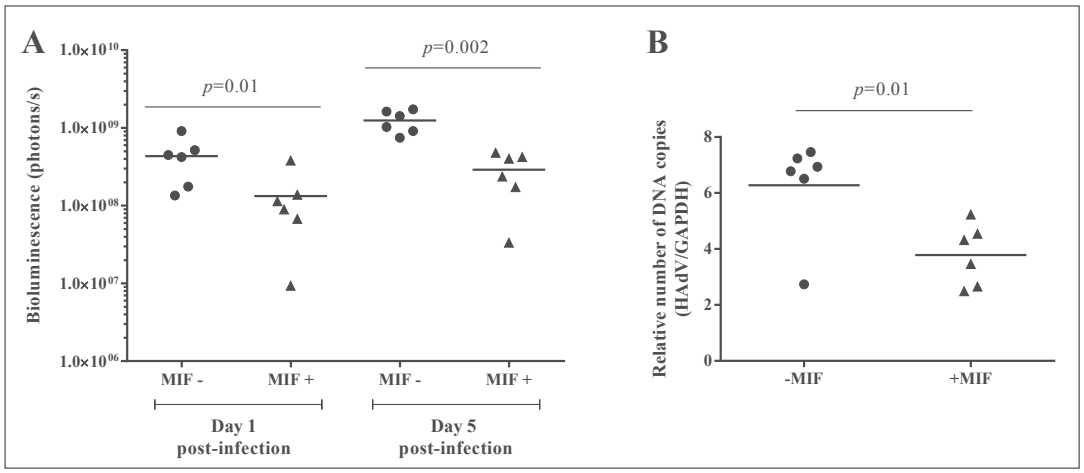

Figure 2. MIF inhibits entry of HAdV in human cells. **A**. Chemical structure of MIF. **B**. Dose-dependent activity of MIF on HAdV5-GFP at high MOI (2,000 vp/cell) in an entry assay. DMSO control corresponds to cells infected at the same MOI but in the absence of drug. The results represent means ± SD of triplicate samples from three independent experiments. **C**. Lack of activity of MIF on HAdV-mediated endosomolysis in a α-sarcin assay, as describe in Methods. Data shows the percentages of HPG incorporation. The results represent means ± SD of triplicate assays.

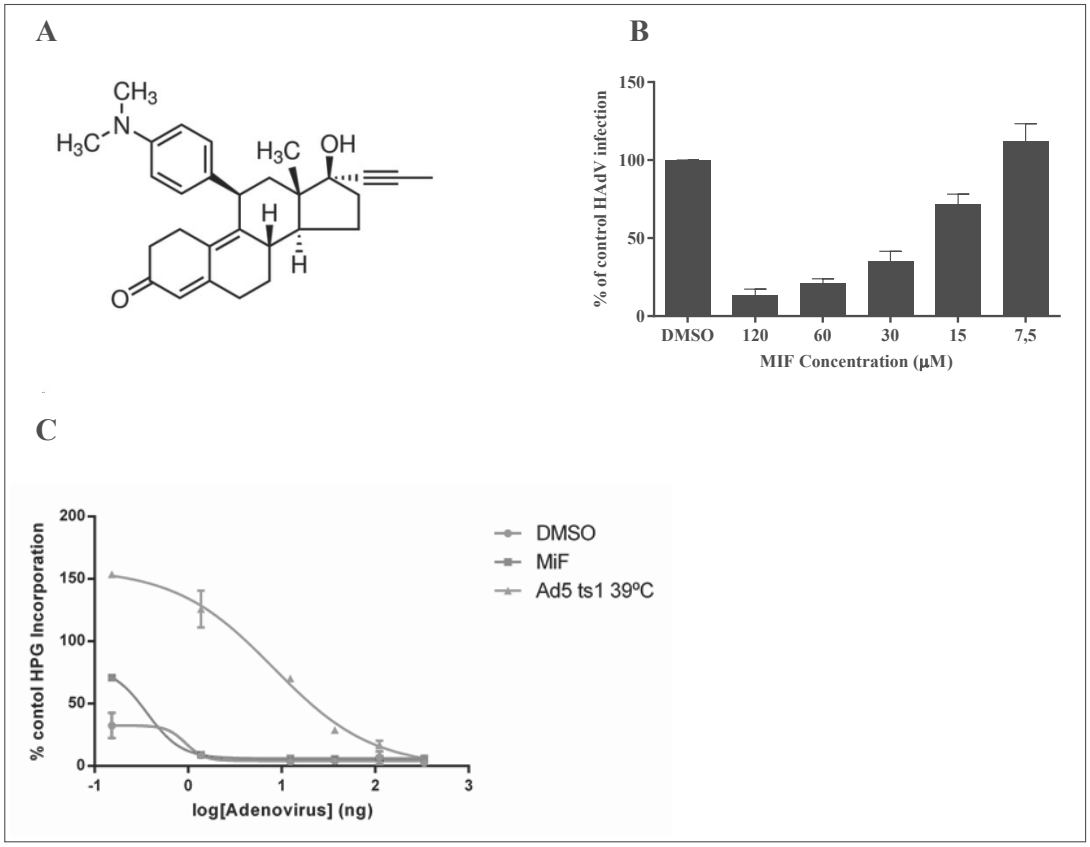

Figure 3. Nuclear association of HAdV5 genome. A) The presence of MIF altered the access of HAdV genomes to the nucleus (*** = $p < 0.001$). B) Control for the specificity of nuclear DNA purification. Bars represent means ± SD of triplicate samples from two independent experiments

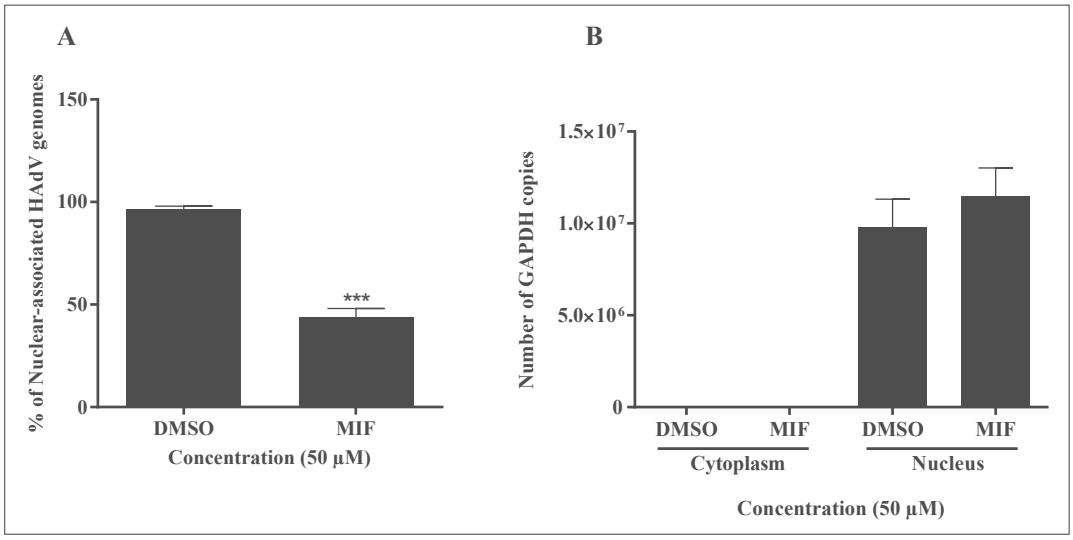

Figure 4. MIF inhibits DNA replication. A) Reduction of *de novo* production of HAdV DNA copies 24 hours post-infection in A549 cells determined by a quantitative PCR assay. B) *De novo* production of HCMV DNA copies was determined 72 hours post-infection by quantitative PCR assay. Results are expressed as the relative copy number of HADV/HCMV DNA normalized to GAPDH copy number and are presented as the mean ± SD from triplicate assays (*** = $p < 0.001$).